International Journal of Fuzzy Logic and Intelligent Systems, vol. 6, no. 2, June 2006 pp. 161-166

Simultaneous Localization and Mobile Robot Navigation using a Sensor Network

TaeSeok Jin*, and Hideki Hashimoto**

***Dept. of Mechatronics Engineering, DongSeo University,**
San 69-1 Churye-2 Dong, Sasan-Gu, Busan 617-716, Korea
****Institute of Industrial Science, University of Tokyo,**
4-6-1 Komaba Meguro-ku Tokyo 153-8505, Japan

Abstract

Localization of mobile agent within a sensing network is a fundamental requirement for many applications, using networked navigating systems such as the sonar-sensing system or the visual-sensing system. To fully utilize the strengths of both the sonar and visual sensing systems, This paper describes a networked sensor-based navigation method in an indoor environment for an autonomous mobile robot which can navigate and avoid obstacle. In this method, the self-localization of the robot is done with a model-based vision system using networked sensors, and nonstop navigation is realized by a Kalman filter-based STSF(Space and Time Sensor Fusion) method. Stationary obstacles and moving obstacles are avoided with networked sensor data such as CCD camera and sonar ring. We will report on experiments in a hallway using the Pioneer-DX robot. In addition to that, the localization has inevitable uncertainties in the features and in the robot position estimation. Kalman filter scheme is used for the estimation of the mobile robot localization. And Extensive experiments with a robot and a sensor network confirm the validity of the approach.

Key Words : Multi-sensor data fusion, Obstacle avoidance, Image processing, Localization, Kalman filter

1. Introduction

For mobile robots to operate efficiently in a human environment, they need to be able to navigate efficiently and to avoid collisions. Therefore, taking the safety factor into consideration, "collision avoidance" would essentially form the basic behavior of all behavior-based autonomous robots. The sonar sensing system has traditionally been used for collision avoidance in mobile robots [1],[2]. It is cost effective and relatively quick in response. Processing is not time consuming either. Recently, however, with the reduction in size of video cameras and the increase in computing speed of computers, the use of visual sensing has become popular too [3],[4].

In what has become a fairly well-researched approach to networked multi-sensor (sonar and vision) based navigation for mobile robots, a robot is provided with an environmental map and a path to follow. The important function of vision-based processing in this case consists of "self-localization." By comparing these prerecorded images with the camera images taken during navigation, the robot is able to determine its location. Other previous research contributions that are relevant to mobile robot localization include [4],[5].

In this paper, we will present an networked multi-sensor based process for mobile robots that is capable of simultaneously navigating and avoiding stationary obstacles using monocular camera images. While the self-localization part of the process is the same as the FINALE system[7], what distinguishes the work reported in this paper is that we are now able to give to the robot a vision-based obstacle avoidance capability at the same time. In the current implementation, this obstacle-avoidance capability is limited to the detection and avoidance of stationary obstacles. This is owing to the limitations of the computing hardware available to the robot. Therefore, moving obstacles must still be detected with ultrasonic sensors.

In this paper, we focused our endeavour on the concurrent network sensor application and localization by adopting the feature representation method and absolute localization method for the robot autonomy. And in the midst of concurrent processing, through the quantification for each process, we showed the performance improvement and systematic relationship between the map building and localization. as a general approach of sensor fusion, and STSF (space and time sensor fusion)[8] scheme is applied for sensor data structure and applied to the landmark identification for mobile robot navigation.

2. Active sensor fusion system

A block diagram of the active sensor fusion system is shown in Figure 1. Basically, there are four modules: the sonar sensor module, the visual module, the situation

Manuscript received May. 31, 2006; revised Jun. 15, 2006.

assessment module and the movement module. These modules are individually sub-divided into sub-modules as shown in table 1. The first two main modules are "sensing modules" and all the data collected by these two modules are relayed to the situation assessment module, which will decide on an appropriate action or reaction (based on past and present data) and which will in turn, pass an order to the movement module[9].

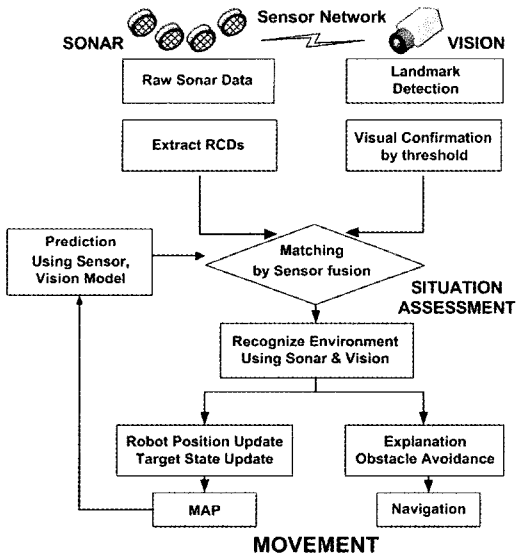

Fig. 1. Active Sensor Fusion System

Table 1. Modules of the sensor fusion system.

Main modules	Sub-modules
Visual	Landmark Detection Visual Confirmation
Sonar	Extract RCDs Sonar Confirmation
Situation Assessment	Matching by Sonar and Vision
Movement	Map building Navigation

3. Localization from the multi-sensor data

3.1 Mobile robot localization

Localization if the process of determining the position of the robot with respect to a global reference frame. Our objective here is to achieve comparable performance to commercially available artificial beacon systems [9] without modifying the environment, by using the naturally occurring structure of the environment.

When the mobile robot starts from the known initial point, in the view of dead reckoning, it collects the data from the motor encoder and angle potentiometer. And then the extracted position information is used to generate virtual map with the simulated RCDs. These simulated RCDs are used together with real RCD data for map matching process. In other words, when the real sonar data is acquired at time step k, the position is estimated for the most similar pattern of virtual RCD and based on that position, the virtual RCD pattern is predicted at time step k+1 and then the real RCD pattern at time step k+1 is compared with the virtual RCD pattern. This routine is continuously processed in chain type as shown in Fig. 3.

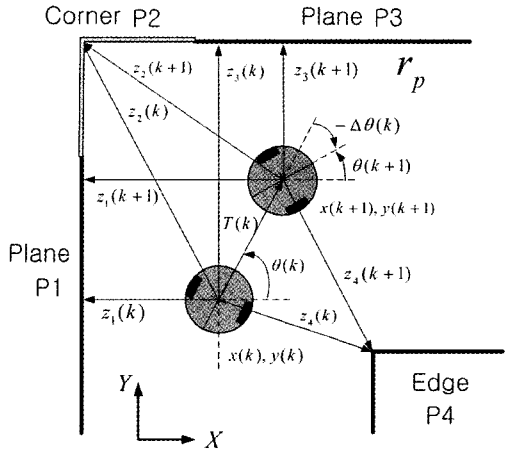

Fig. 2. Localization using Measured and Predicted Data

With reference to Figure 2, the vector $x(k)=(x(k), y(k), \theta(k))$ is the robot's position and angle at time k. Four geometric beacons are in view to a servo-mounted sonar at time k and time k+1: plane $\mathbf{P}_1$, corner $\mathbf{P}_2$, plane $\mathbf{P}_3$ and cylinder $\mathbf{P}_4$. The sonar measurements $\mathbf{z}_1(k)$ and $\mathbf{z}_3(k)$ are the shortest distance from the sensor to planes $\mathbf{P}_1$ and $\mathbf{P}_3$ at time k. the measurement $\mathbf{z}_2(k)$ is the distance from the sensor to corner $\mathbf{P}_2$ at time k. Measurement $\mathbf{z}_4(k)$ is the distance to the central axis of cylinder $\mathbf{P}_4$ less the radius of the cylinder.

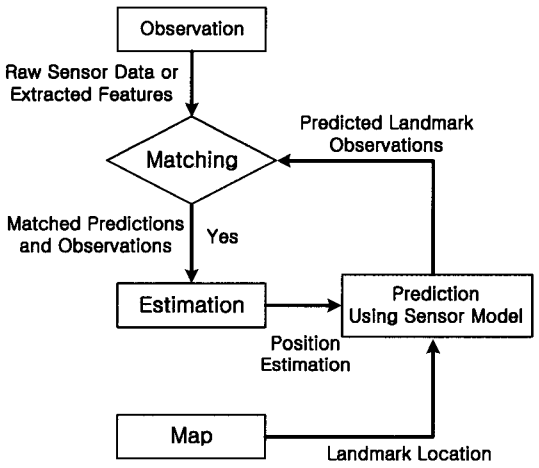

Fig. 3. Localization Process Chained with Map Building

In the localization process, we adapted the Extended Kalman Filter. The position and angle of the robot can be described $\mathbf{x}(k)=(x(k), y(k), \theta(k))^T$ as shown in Fig. 2. Initially the robot starts from the known position with the prior modelled information about the geometric environment features

$\{ \mathbf{p}_t \mid 1 \le t \le n_T \}$ and acquires the measured data $\mathbf{z}_j(k+1)$every sampling time. The purpose of the EKF for the localization is to compute the updated estimate $\hat{\mathbf{x}}(k+1|k+1)$ from the information of environment features $\mathbf{P}_t$ and measured sensor data $\mathbf{z}_j(k+1)$. Generally Kalman Filter is based on 2 models, plant model and measurement model.

3.2 Sensor Fusion Transformation

Let us define the k-th moment data set provided by i-th sensor as, $\mathbf{z}_i(k)$, and the k-th measurement vector as x(k). Then the conventional sensor fusion technique provides the measurement as

$$\hat{\mathbf{x}}(k) = \sum_{i=0}^{n} \mathbf{W}_i \, \mathbf{x}_i(k) \tag{1}$$

where $\mathbf{x}_i(k) = \boldsymbol{H}_i \, \mathbf{z}_i(k) \in \boldsymbol{R}^m$,,

H_i represents transformation from the sensory data to the measurement vector, and $W_i \in R^{m \times m}$ represents the weighting value for i-th sensor.

Note that in the measurement of $\mathbf{z}_i(k)$, the low-level fusion might be applied with multiple sets of data with known statistics[8]. The determination of H_i is purely dependent on the sensory information and the decision of W_i can be done through the sensor fusion process. Later this measured data are provided to the linear model of the control/measurement system as current state vector, $\mathbf{x}(k)$. In this approach, we propose a multi-sensor data fusion using sensory data, $Tz_i(j)$, as

$$\hat{\mathbf{x}}(k) = \sum_{i=1}^{n} \mathbf{W}_i \left\{ \sum_{j=1}^{k} P_j T z_i(j) \right\} \tag{2}$$

where $\sum_{j=1}^{k} P_j = 1$.

Note that when each of sensor information can provide the measurement vector, that is, the redundant case, $Tz_i(j)$ can be expanded as

$$Tz_i(j) = T_j + H_i z_i(j) \tag{3}$$

where T_j represents the homogeneous transformation from the location of the j-th to the k-th measurements.

However, when the multi-sensors are utilized in the complementary mode, the transformation relationship cannot be defined uniquely; instead it will be defined depending on the data constructing algorithm from the measurements. For example, a single image frame captured by a camera on a mobile robot cannot provide the distance to an object until the corresponding object image is provided again from a different location. Fig. 4 illustrates the concept of this multi-sensor temporal data fusion. Estimation of parameter may provide the measurement vector at each sampling moment.

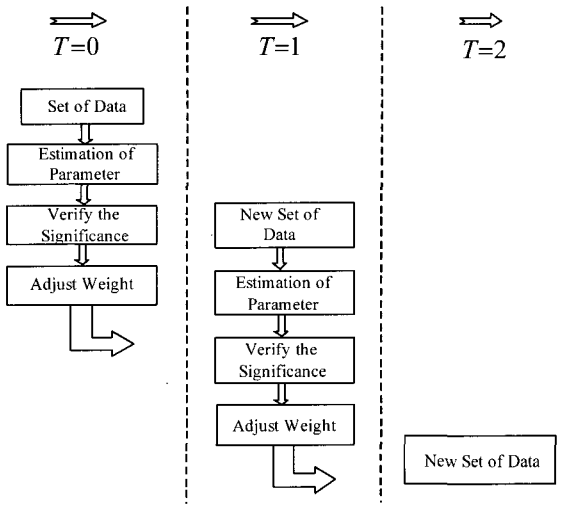

Fig. 4 Concept of Space and Time Sensor Fusion

3.3 Robot Position Prediction

First, using the plant model and knowledge of the control input $\mathbf{u}(k)$, we predict the robot's new location at time step k+1.

$$\hat{\mathbf{x}}(k+1|k) = \mathbf{f}(\hat{\mathbf{x}}(k|k), \mathbf{u}(k)), \tag{4}$$

We next compute $\mathbf{P}(k+1|k)$, the variance associated with this prediction:

$$\mathbf{P}(k+1|k) = \nabla \mathbf{f} \, \mathbf{P}(k|k) \, \nabla \mathbf{f}^T + \mathbf{Q}(k) \tag{5}$$

where, $\nabla \mathbf{f}$ is the Jacobian of the state transition function $\mathbf{f}(\hat{\mathbf{x}}(k|k), \mathbf{u}(k))$ obtained by linearizing about the updated estimate $\hat{\mathbf{x}}(k|k)$.

$$\nabla \mathbf{f} = \begin{bmatrix} 1 & 0 & -T(k)\sin(\hat{\theta}(k|k)) \\ 0 & 1 & T(k)\cos(\hat{\theta}(k|k)) \\ 0 & 0 & 1 \end{bmatrix} \tag{6}$$

The next step is to obtain the observation set Z(k+1) from the vehicle's sensors from the new vehicle location. This is comprised of n_0 observed RCDs. Next, for each sensor we use the predicted robot location $\hat{\mathbf{x}}(k+1|k)$ and the current map M(k) to generate predicted observations of each target P_t :

$$\hat{\mathbf{z}}_i(k+1) = \mathbf{h}_{st}(\mathbf{p}_t, \hat{\mathbf{x}}(k+1|k), \mathbf{b}_s), \quad i = 1, \ldots, n_p \tag{7}$$

to yield the set of predictions

$$\hat{\mathbf{Z}}(k+1) = \{ \hat{\mathbf{z}}_i(k+1) \mid 1 \le i \le n_p \} \tag{8}$$

which contains n_p predicted RCDs. The predicted state estimate $\hat{\mathbf{x}}(k+1|k)$ is used to compute the measurement Jacobian $\nabla \mathbf{h}_i$ for each prediction. For planes,

$$\nabla \mathbf{h}_i = pv \begin{bmatrix} -\cos(p_\theta) \\ -\sin(p_\theta) \\ x'_s \sin(\hat{\theta}(k+1|k) - p_\theta \\ -y'_s \cos(\hat{\theta}(k+1|k) - p_\theta) \end{bmatrix}^T \quad (9)$$

while for corners, and edges

$$\nabla \mathbf{h}_i = \frac{-1}{d} \begin{bmatrix} \hat{x}(k+1|k) + x'_s \cos(\hat{\theta}(k+1|k)) \\ -y'_s \sin(\hat{\theta}(k+1|k) - p_x) \\ \hat{y}(k+1|k) + x'_s \sin(\hat{\theta}(k+1|k)) \\ -y'_s \cos(\hat{\theta}(k+1|k) - p_y) \\ 0 \end{bmatrix}^T \quad (10)$$

where, d is the distance from the predicted location of sensors to the point (p_x, p_y).

3.4 Matching and Estimation

The goal of the matching procedure is to produce an assignment from measurements $\mathbf{z}_j(k)$ to targets $\mathbf{p}_t$. For each prediction and observation corresponding to the same sensor s, we first compute the innovation $v_{ij}(k)$.

$$\begin{aligned} v_{ij}(k+1) &= [\ \mathbf{z}_j(k+1) - \hat{\mathbf{z}}_i(k+1)] \\ &= [\ \mathbf{z}_j(k+1) - \mathbf{h}_i(\ \mathbf{p}_t,\ \hat{\mathbf{x}}(k+1|k))] \end{aligned} \quad (11)$$

If prediction i and observation j correspond to different sensors, the innovation $v_{ij}(k+1)$ is set to infinity. The innovation covariance can be found by linearizing Equation (3) about the prediction, squaring, and taking expectations to yield

$$\begin{aligned} \boldsymbol{S}_{ij}(k+1) &\equiv E[v_{ij}(k+1) v_{ij}^T(k+1)] \\ &= \nabla \mathbf{h}_i\ \mathbf{P}(k+1|k)\ \ \nabla \mathbf{h}^T{}_i(k+1) + \boldsymbol{R}_i(k+1) \end{aligned} \quad (12)$$

A validation gate is used to determine the correspondence between predictions and observations [10]:

$$v_{ij}(k+1)\ \ \boldsymbol{S}_{ij}^{-1}(k+1) v_{ij}^T(k+1) \le g^2 \quad (13)$$

This equation is used to test each sensor observation $\mathbf{z}_i(k+1)$ for membership in the validation gate for each prediction measurement. When a single observation falls in a validation gate, we get a successful match.

The final step is to use successfully matched predictions and observations to compute $\hat{\mathbf{x}}(k+1|k+1)$, the updated robot location estimate. To do so we use a parallel update procedure [11]. We first stack the validated measurements $\mathbf{z}_j(k+1)$ into a single vector to form $\mathbf{z}(k+1)$, the composite measurement vector for time k+1, and designate the composite innovation $v(k+1)$. Next, we stack the measurement Jacobians $\nabla \mathbf{h}_i$ for each validated measurement together to form the composite measurement Jacobian $\nabla \mathbf{h}$. Using a stacked noise vector $\mathbf{R}(k+1) = diag[\ \mathbf{R}_j(k+1)]$, we then compute the composite innovation covariance $\mathbf{S}(k+1)$ as in eq. (12). We then utilize the well-known result [10] that the Kalman gain can be written as

$$\boldsymbol{W}(k+1) \equiv \mathbf{P}[v_{ij}(k+1|k)\ \nabla \mathbf{h}^T S^{-T}(k+1)] \quad (14)$$

to compute the updated robot position estimate

$$\hat{\boldsymbol{x}}(k+1|k+1) = \hat{\boldsymbol{x}}(k+1|k) + \boldsymbol{W}(k+1) v(k+1) \quad (15)$$

with associated variance

$$\begin{aligned} \mathbf{P}\ (k+1|k+1) = \mathbf{P}(\mathrm{k}+1\ |\mathrm{k}) \\ -\ \mathbf{W}\ (k+1)\ \mathbf{S}(k+1)\ \boldsymbol{W}^T(k+1) \end{aligned} \quad (16)$$

4. Experiments setup and results

4.1 Mobile robot system and environment

After satisfactory simulation performance, the proposed navigation control system has been implemented and tested in a laboratory environment on a Pioneer-DX robot equipped with a CCD camera and ultrasonic sensor ring (Fig. 5) [11]. This robot, which is manufactured by ActivMedia Robotics, is a differentially driven platform configured with two drive wheels and one swivel caster for balance. Each wheel is driven independently by a motor with 19.5:1 gear ratio which enables the robot to drive at a maximum speed of 1.2 m/s and climb a 25% grade. The proposed system was prepared using fuzzyTECH software, which generated C++ code that was implemented on the Pioneer-DX [11].

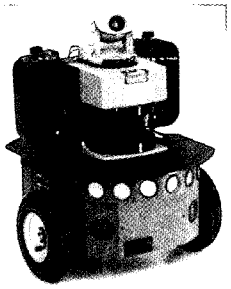

Fig. 5. Pioneer-DX Mobile Robot and Active Camera System

Ultrasonic sensor is good in distance measurement of the obstacles, but it also suffers from specular reflection and insufficient directional resolution due to its wide beam opening-angle. So, we use a sensor fusion method to decide the distance and width of obstacles and avoid them during the navigation. Pioneer-DX examines whether measured value is data of distance to real obstacle or distance to its shadow. If difference of measured data by vision and ultrasonic sensor is within the error tolerance, Pioneer-DX uses measured data by vision sensor as distance to obstacle. Otherwise, Pioneer-DX uses measured data by vision sensor as distance to obstacle. Fig. 6 depicts sensing coverage of vision and ultrasonic sensor used this experiment. Ultrasonic sensor can detect obstacles within 7m and Vision system can detect obstacles within the range of between 130cm and 870cm.

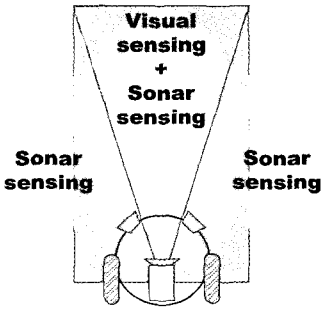

Fig. 6. Sensing Coverage of Vision and Ultrasonic Sensor

4.2 Mobile robot Navigation

Kalman-based STSF have first been tested with experiment to show the usefulness of proposed method in two environments case 1, case 2 respectively. Starting at (0.3m, 5m, 0 degree), a virtual robot was driven around a virtual square corridor one time. The walls in the artificial environment are denoted by the real map, IRL corridor of PNU.

In each round, the robot stops a total of 12 times to rescan the environment. The size of given map is 12m X 8m, the total distance traveled is 12 + 8=20 meters, and the total number of scanning points is 38. The position and the direction of navigation at all stops is shown in Fig. 7. This result demonstrates one of many successful experiments. The algorithm is very effective in escaping local minima encountered in laboratory environments. And the results are compared to show the superiority of the proposed scheme. The robot was allowed to move keeping the distance between robot and obstacles constant at the region, AT and BT. The region BT, shows the improvement in steering at corner. And the simulation experiments show that a mobile robot, utilizing our scheme, can avoid obstacles and reach a given goal position in the workspace of a wide range of geometrical complexity. Experiments results using Kalman-based STSF, show the robot can avoid obstacles (boxes and trash can) and follow the wall.

The mobile robot navigates along a corridor with 3m width and with some obstacles as shown in Fig. 7. It demonstrates that the mobile robot avoids the obstacles intelligently and follows the corridor to the goal. Also notice that especially at the region AT, the errors of the robot position converse to zero as the same reason, referring to the simulation result and experimental result in Fig. 7(a) and Fig. 7(b) represent the reference of robot direction produced by the proposed Kalman-based STSF. Finally, the robot is tested to follow the whole trajectory from start position to final position as shown in Fig. 7. The simulation and experimental results of the robot status under such control strategy are given in Fig. 8 and Fig. 9.

As compared to Fig. 8, the response of the position is reasonably smooth, whereas the orientation θ continues to be very noisy during the sampling step 30. This is due to distortions of the images caused by the brightness of light and sonar reflection's noise from wall. During the sampling step of 90 ms, the position error is at most 120 mm, and the orientation error is up to 10 degrees.

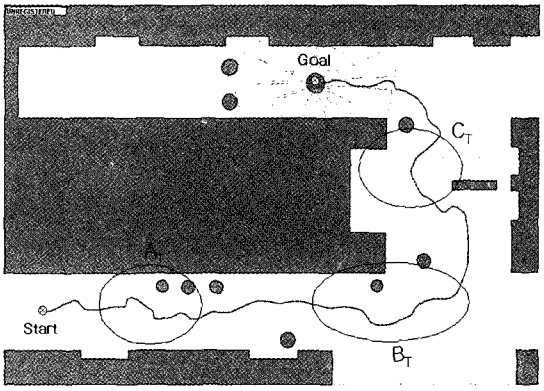

(a) Navigation in a corridor, case 1

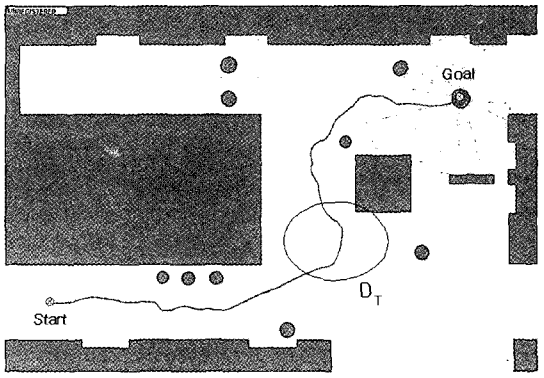

(b) Navigation in a corridor, case 2

Fig. 7. Experiment Results used Sensor Network

In future research efforts, it is necessary to examine the influence of the mobile robot, which maintains a flexible distance between the robot and the obstacles. In the environment such as factory and office, since a walking-human trajectory is newly generated at every step, it is considered to be a function of time. Therefore, the application of navigation control is effective.

5. Conclusions

In this paper, we have presented a sensor fusion-based navigational system with ultrasonic sensor and vision sensor for mobile robots that is also capable of avoiding at least the stationary obstacles using vision data and tested it experimentally on an IRL-2001 mobile robot. By using a combination of model-based vision for self-localization; position updating to cope with the time delays associated with landmark image processing; using vision data for not only self-localization but also for the calculation of directions of safe passage in the presence of obstacles; and ultrasonic sensors for the detection of close-range moving obstacles; we have created a navigational system that makes optimum use of all the sensors for smooth and continuous navigation in indoor environments. Based on these results, further experiments will aim at applying the proposed tracking technique to the multi-sensor fusion scheme which is applied to the control of

a mobile robot in an unstructured environment. The Kalman-based STSF will be applied for conducting on landmark based real-time robot guidance, including visual servo control of the Pioneer-DX mobile robot for autonomous navigation.

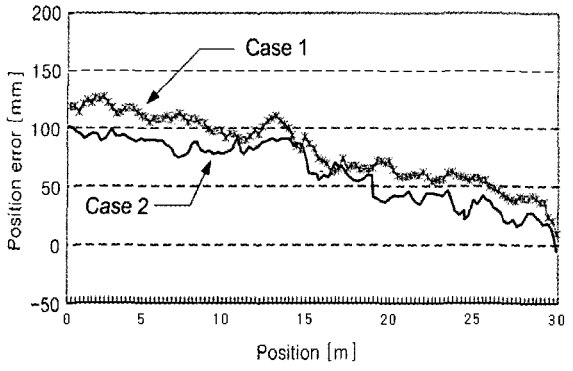

Fig. 8. Robot Position Error

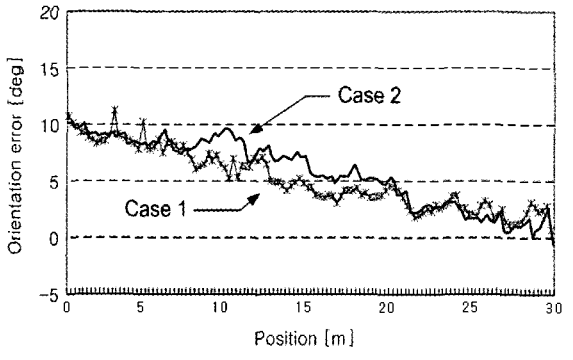

Fig. 9. Robot Direction Error

References

[1] Y. Nakamura, "Nonholonomic robot system, Part 2: Motion planning under kinematic nonholonomic constraints," J. Robot. Soc. Jpn., vol. 11, no. 5, pp. 655-662, 1993.

[2] J. Borenstein and Y. Koren, "Histogramic in-motion mapping for mobile robot obstacle avoidance," IEEE Trans. Robot. Automat., vol. 7, pp. 535-539, Aug. 1991.

[3] T. Camus, D. Coombs, M. Herman, and T. Hong, "Real-time singleworkstation obstacle avoidance using only wide-field flow divergence," in Proc. 13th Int. Conf. Pattern Recog., Aug. 1996.

[4] J.-H. Lee, G. Appenzeller, and H. Hashimoto, "An agent for intelligent spaces: Functions and roles of mobile robots in sensored, networked, thinking spaces," in Proc. IEEE Conf. Intelligent Transportation Systems, Boston, MA, pp. 983-988, 1997.

[5] M. Devy and H. Bulata, "Landmark-based vs. feature-based localization of a mobile robot in a structured environment," in Proc. Int. Conf. Adv.Robot., 1995.

[6] A. Kosaka and A. Kak, "Fast vision-guided mobile robot navigation using model-based reasoning and prediction of uncertainties," CVGIPImage Understanding, vol.56, no.3,

[7] A. Kosaka and J. Pan, "Purdue Experiments in Model-based Vision for Hallway Navigation", in Proc. of Workshop on Vision for Robots in IROS'95, pp.87-96, 1995.

[8] T. S. Jin, J. M. Lee, and S. K. Tso, "A New Space and Time Sensor Fusion Method for Mobile Robot Navigation" Journal of Robotic Systems, Vol. 21, No. 7, pp. 389-400, 2004

[9] J.-H. Lee and H. Hashimoto, "Mobile robot control by distributed sensors," in Proc. IFAC Workshop Mobile Robot Technology, pp. 85-90, 2001.

[10] John J. Leonard and Hugh F. Durrant-Whyte. "Direct Sonar Sensing for Mobile Robot Navigation," Kluwer Academic Publisher, 1992.

[11] Pioneer-DX. ActivMedia Robotics, Amherst, NH. [Online]. Available: http://www.activmedia.com/

TaeSeok Jin

He received the Ph.D. degrees from Pusan National University, Busan, Korea, in 2003, in electronics engineering.

He is currently a full-time lecturer at Dongseo University. From 2004 to 2005, he was a Researcher at the Institute of Industrial Science, The University of Tokyo, Japan. His research interests include Network sensors data fusion, mobile robots, computer vision, and intelligent control. Dr. Jin is a Member of the KFIS, IEEK, ICASE, and JSME.

Phone : +82-51-320-1541
Fax : +82-51-320-1751
E-mail : jints@dongseo.ac.kr

Hideki Hashimoto (S'83-M'84)

He received the B.E., M.E., and Dr.Eng. degrees in electrical engineering from The University of Tokyo, Tokyo, Japan, in 1981, 1984, and 1987, respectively.

He is currently an Associate Professor at the Institute of Industrial Science, The University of Tokyo. His research interests are control and robotics, in particular, advanced motion control and intelligent control. Dr. Hashimoto is a Member of the Society of Instrument and Control Engineers of Japan, Institute of Electrical Engineers of Japan, and Robotics Society of Japan

Phone : +81-3-5452-6258
Fax : +81-3-5452-6259
E-mail : hashimoto@iis.u-tokyo.ac.jp